Int. J. Solids Structures, 1968, Vol. 4, pp. 175 to 196. Pergamon Press. Printed in Great Britain

GENERALIZED PYRAMIDAL FRACTURE AND YIELD CRITERIA

B. PAUL

Ingersoll-Rand Research Center, Princeton, New Jersey

Abstract—The generalized pyramidal failure criterion is shown to be a convenient criterion for describing the state of stress under which isotropic materials will yield or undergo brittle fracture. The generality of the criterion is useful for very complex materials, but it is believed that most materials can be adequately described by simple variants of the general criterion. For example, it is shown that the hexagonal pyramid criterion, a special case of the more general pyramidal criterion, is capable of describing a very broad range of material behavior through the use of only three experimentally determined parameters. The application of the pyramidal criteria to real materials is illustrated in a review of experimental results on brittle metals, concretes, natural rocks, granular materials, and soils.

1. INTRODUCTION

MATERIAL behavior under time-independent, isothermal conditions can be classified as ductile at one extreme and brittle at another extreme, while many materials can be made to undergo a transition* from the ductile state to the brittle state or vice-versa. By definition, all materials "in the ductile state" will undergo *yielding* before they ultimately fracture. Those combinations of stress components which result in initial yielding of such materials are defined by a *yield criterion*

$$f(\sigma_{ij}; C_1, C_2, \ldots) = 0 \tag{1.1}$$

where σ_{ij} ($i = 1, 2, 3$) are stress components referred to an arbitrary cartesian coordinate system x_i, and C_1, $C_2, \ldots$ etc., are constants which presumably can be determined by means of suitable experiments. Materials will be said to be in a "brittle state" if fracture takes place before any appreciable plastic flow occurs. For such materials an equation, of the form (1.1), may exist which defines all those combinations of stress components which will cause fracture; such an equation, if it exists, defines a *fracture criterion.*

Although initially ductile metals will usually† fracture if loading is continued beyond initial yield (ductile fracture), there is no evidence available that an equation of type (1.1) can be used to predict the final state of stress at which these metals will fracture. It is known that the path of loading and the strain history play a large role in the ductile fracture process, for the case of arbitrary (non-proportional) loading.

Thus, we see that it is certainly meaningful to seek *yield criteria* for materials in the ductile state and *fracture criteria* for materials in the brittle state, but we should not expect

* It is known that the same material may be in the brittle or ductile state, depending upon such factors as temperature, pressure, rate of loading, etc. Thus, strictly speaking we should speak of the "brittle state" or "ductile state" of materials, rather than of "brittle materials" or "ductile materials" [1, p. 207]. Nevertheless, we shall, for the sake of brevity, occasionally use the latter designations whenever no confusion seems likely to arise.

† Virtually unlimited ductility has been observed in the presence of very high hydrostatic pressure fields.

a universal *failure criterion* to simultaneously describe yielding, brittle fracture, and ductile fracture.

Our present knowledge of initial yield criteria for isotropic ductile materials is quite good, and fortunately these yield criteria are of a reasonably simple nature. However, our state of knowledge on brittle materials (including ceramics, rocks, soils, and granular media, as well as brittle metals) is relatively imperfect. Furthermore, the variety of admissible fracture criteria for brittle materials would, on the surface, seem to be very much greater and much more complex than the few simple criteria which govern yielding of ductile materials.

In this paper we seek to show that most of the fracture criteria which have been proposed over the past years can be viewed as special cases of a particular fracture criterion which we will refer to as the *generalized pyramidal failure criterion.* Although it is our intention to apply this generalized criterion mainly to *fracture,* we call it a *failure* criterion because it can represent, with suitable accuracy, any equation of the form (1.1), whether it be interpreted as a yield or fracture criterion.

Of course, unlimited generality, in itself, is not necessarily of great value. But, when it turns out that the *simplest* variants of a very general criterion, can describe, with great accuracy, an extremely wide class of experimental observations, then the simpler variants of the general criterion become a valuable working tool. We will show that the simplest variant of the generalized pyramidal criterion, which we refer to as the *hexagonal pyramid failure criterion,* can correlate the greatest bulk of available experimental evidence on brittle metals, rocks, and soils. Not only does the inherent simplicity of this three-parameter piecewise-linear failure criterion make it mathematically attractive, but specialization of the material parameters reduces the hexagonal pyramid criterion to the well known Coulomb–Mohr criterion which has already been demonstrated to have a wide (though not unlimited) range of application for soils [2, 3], rocks [4], and other brittle materials [5]. Although some pertinent past work is described in these papers, more comprehensive reviews will be found in standard works such as Nadai's [1], and in a forthcoming chapter by Paul [6].

In the next section, we briefly discuss the *pressure-independent* class of yield criteria which are suitable for ductile metals, but are inadequate for brittle materials. In Section 3, a generalized *pressure-dependent* criterion, called a *pyramidal failure criterion,* is described, and a specialized case, the *hexagonal pyramid criterion,* is described in the next section. In Section 5, it is shown that a great many of the yield and fracture criteria proposed in the past are special cases of the pyramidal criterion. In the next Section, it is shown how the pyramidal criterion correlates experimental results for brittle metals, granular materials such as soils, concrete, and natural rocks. Conclusions are stated in Section 7.

2. FAILURE SURFACES FOR PRESSURE-INDEPENDENT MATERIALS (YIELDING OF METALS)

Since any stress component σ_{ij} can be expressed in terms of the three principal stresses $\sigma_1, \sigma_2, \sigma_3$, and three angles which define the principal directions in physical space, the failure criterion (1.1) can be expressed in terms of three principal stresses and three angles rather than in terms of six stress components referred to an arbitrary coordinate system. The directions of principal axes cannot influence the yielding of an isotropic material (this may be considered a definition of isotropy, if desired), therefore the criterion of failure can be expressed in the form

$$f(\sigma_1, \sigma_2, \sigma_3; C_1, C_2, \ldots C_n) = 0. \tag{2.1}$$

Equation (2.1) may be thought of as the equation of a surface in a stress space with cartesian coordinates $\sigma_1, \sigma_2, \sigma_3$; this surface is called the *failure surface* (sometimes *fracture surface*, or *yield surface*, where applicable). It is easily shown [7, p. 17], that if the failure criterion is independent of the presence, or absence, of an overall hydrostatic pressure (or tension), then the failure surface must be a cylinder whose generators are all parallel to the *hydrostatic axis*. The hydrostatic axis is hereby defined to be a straight line through the origin in stress space, which makes the same angle α ($\cos\alpha = \frac{1}{\sqrt{3}}$; $\alpha = 54{\cdot}8°$) with each coordinate axis. This type of failure surface will be called a *pressure-independent* failure surface, and is characteristic of the yielding of ductile metals [1, 7], but is not characteristic of fracture in brittle materials [2, 4, 5] and [8, p. 457].

Nevertheless, it is worth spending a moment to explore the possible shapes of pressure-independent failure surfaces. In particular, we will wish to note similarities and differences between these surfaces and those which are more relevant for brittle materials.

If we view the failure cylinder along the hydrostatic axis, we will see a right section of the cylinder which is the intersection of any *equipressure plane* with the cylinder. An equipressure plane is defined to be any plane which is perpendicular to the hydrostatic axis, and is thus described by the equation:

$$\sigma_1 + \sigma_2 + \sigma_3 = \text{constant}. \tag{2.2}$$

When the constant in equation (2.2) is zero, the equipressure plane passes through the origin and will be referred to as the *deviatoric plane*. This nomenclature is suggested by the fact that any stress point $P(\sigma_1, \sigma_2, \sigma_3)$ in stress space defines a vector $\overline{OP}$ from the origin O to the point P. This vector may be resolved into a component $\overline{ON}$ along the hydrostatic axis and a component $\overline{OQ}$ perpendicular to it. The latter component may be shown [7, p. 17] to have components along the coordinate axes, S_1, S_2, S_3 given by

$$(S_1, S_2, S_3) = (\sigma_1 - \sigma_m, \sigma_2 - \sigma_m, \sigma_3 - \sigma_m)$$

where

$$\sigma_m = (\tfrac{1}{3})(\sigma_1 + \sigma_2 + \sigma_3).$$

The components S_1, S_2, S_3 of $\overline{OQ}$ are the principal components of the stress deviator tensor, therefore it is convenient to refer to the plane in which vector $\overline{OQ}$ lies, as the deviatoric plane.

Figure 1 shows two possible cross-sections of the yield surface in the deviatoric plane. The axes σ_1', σ_2', σ_3' are the projections of the coordinate axes on the deviatoric plane. The cross-sections (or "loci", as they will be referred to henceforth) would fully define a cylindrical failure surface but would merely define one of an infinite number of *equipressure cross-sections* for a more general failure surface. In any case, isotropy requires the threefold type of symmetry shown in Fig. 1, because an interchange of the arbitrarily numbered coordinate axes could not influence the failure surface for an isotropic material. Threefold symmetry requires that the failure locus need only be given in any one of the sixty-degree sectors I–VI, in Fig. 1, in order for the complete locus to be uniquely specified.

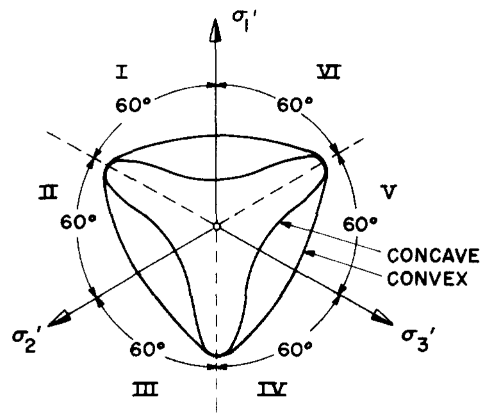

FIG. 1. Projection on deviatoric plane of cross-section normal to hydrostatic axis.

In the case of ductile metals, it may be argued on the basis of extremely plausible assumptions [9, 10], that the yield surface must be convex when viewed from outside (i.e. concave when viewed from the origin). In addition, it has been found experimentally, that the yield points in tension and compression are essentially equal for mildly annealed ductile metals. It is readily seen that all convex loci showing threefold symmetry and equal strength in tension and compression must lie between the two hexagons shown in Fig. 2.

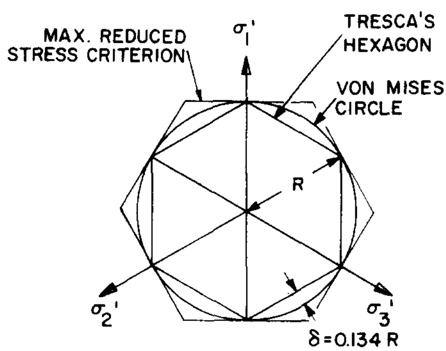

FIG. 2. Tresca's and Von Mises' yield loci matched in tension.

A particularly simple yield locus, which lies between the two hexagons, is the circle shown in Fig. 2. The inner hexagon represents Tresca's [11] maximum shear stress criterion of failure, and the circle represents Von Mises' [12] criterion*. Experimental points for ductile metals usually fall between the Tresca and Mises loci, with the latter giving a slightly better correlation (see Hill [7, p. 21], [16, 17, 18]).

Although no physical justification has been advanced for adopting the circumscribing hexagon of Fig. 2, it was recognized as an outer bound, for convex loci, by Ivlev [19], and

* Although we do not wish to trace out the historical development of any failure criterion, it should be mentioned that in addition to Von Mises, many others have given reasons for adopting the same yield criterion. These others include Maxwell [13] Huber [14], Hencky [15], Nadai [16].

its corresponding criterion has been dubbed the "maximum reduced stress criterion" by Haythornthwaite [20]. It is indicated in Fig. 2 that Tresca's hexagon departs from Mises' circle by at most 13·4%, when both criteria predict the same uniaxial tensile strength, but the maximum deviation can be decreased to 6·7% if the two criteria are matched at some other experimentally observable point, as shown in Fig. 3. Similar adjustments can be made for the circumscribing hexagon.

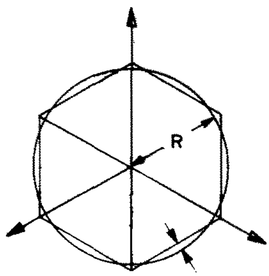

FIG. 3. Tresca's and Von Mises' yield loci matched to minimize δ.

In many problems it is much more convenient to use Tresca's hexagon (or some other approximating polygon) than it is to use Von Mises' circle because the equation of the latter locus is nonlinear in $\sigma_1, \sigma_2, \sigma_3$, whereas the equations of the former locus are linear in each of six sectors of stress space; that is they are "piecewise linear". We could, if we wished to, approximate Von Mises' circle by a regular polygon of any number of sides with ever increasing accuracy.

Cylindrical failure surfaces have been experimentally confirmed only for ductile metals. We will therefore turn our attention to a class of failure surfaces, which are applicable to brittle materials.

3. GENERALIZED PYRAMIDAL FAILURE SURFACES FOR ISOTROPIC MATERIALS

We now consider a class of materials, which are sensitive to the presence of a hydrostatic pressure field. We also allow for the possibility that failure strength in tension and compression may be appreciably different. By thus broadening the allowable behavior, we introduce the possibility of describing the known behavior of brittle metals, rocks, soils, etc. We still, however, observe the restriction of strict isotropy.

The condition of isotropy requires that any equipressure* cross-section of the failure surface must show the threefold type of symmetry depicted in Fig. 1. The innermost locus shown in Fig. 1 is concave in some regions and is therefore not possible for the class of materials known as *stable, work-hardening materials* [9]. However, if we are concerned with *fracture* or with the failure of granular media, rather than with plastic *flow*, there may well exist materials which are not stable work-hardening in the sense of Drucker [9].

* Recall that an "equipressure cross-section" is defined as a section which is perpendicular to the hydrostatic axis.

Different cross-sections of the same failure surface may differ in size and shape depending upon their distance from the origin.

Because of the wide variety of possible failure surfaces, and the analytic complexities associated with many of them, it is logical to explore the simplifications which will result if we approximate a general nonlinear failure surface by an approximating surface which consists of a set of planes which hug the curved surface to any degree of accuracy desired. In other words, we can represent the failure surface by a piecewise linear surface, or polyhedron.

Piecewise linear yield criteria have been explored in the theory of plasticity by numerous writers, including Prager [21, 22], Koiter [23], Sanders [24], Hodge [25], Shield and Ziegler [26], Perrone and Hodge [27], Berman and Hodge [28], and Paul [29]. These writers have been concerned mainly with work-hardening effects, stress-strain relations, and the general theory of limit analysis.

In the case of soils [2], rocks [4], and other brittle materials [5] it has often been the practice to assume *a priori* that the failure surface is indeed the piecewise linear surface of Coulomb–Mohr. The Coulomb–Mohr criterion (a special case of the generalized fracture surfaces under discussion, here) is severely limited in its capacity to represent a sufficiently wide variety of materials because it has only two adjustable parameters, and is completely independent of the intermediate principal stress $\sigma_{\rm II}$. Haythornthwaite's generalization of Coulomb–Mohr theory [20] admits an effect of $\sigma_{\rm II}$, but is restricted to convex hexagonal pyramids.

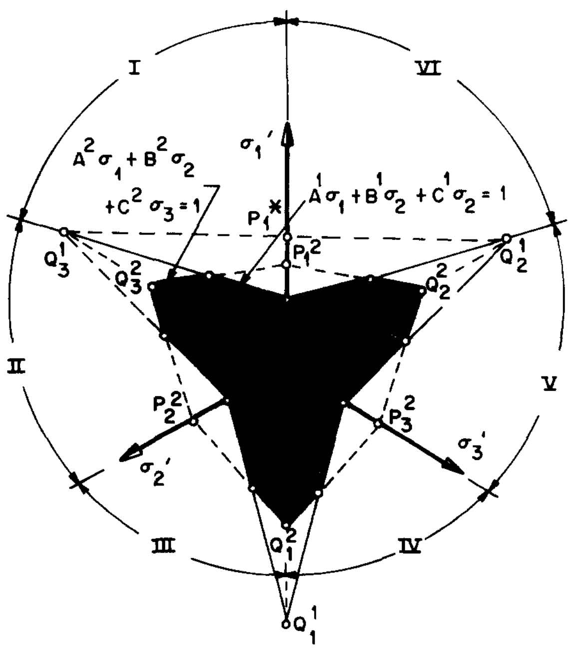

FIG. 4. Twelve-sided cross section of generalized pyramidal failure surface.

The twelve sided polygon shown shaded in Fig. 4 represents a typical cross-section (or level curve), on an arbitrary equipressure plane, for a representative piecewise linear failure surface. Each of the twelve sides is an intersection of the equipressure plane with an oblique plane represented by an equation of the form

$$A\sigma_1 + B\sigma_2 + C\sigma_3 = 1. \tag{3.1}$$

Although there are twelve sides, the thirty-six constants of type A, B, C are not all independent. It may be seen from Fig. 4 that the cross-section is actually the intersection of two hexagons each of which is completely defined by any one of its six sides.

In particular, consider the star shaped hexagon with vertices P_1^1, P_2^1, P_3^1 on the positive axis, and vertices Q_1^1, Q_2^1, Q_3^1 on the negative axes*. Suppose that $P_1^1Q_3^1$ is the trace of an oblique plane whose equation is

$$A^1\sigma_1 + B^1\sigma_2 + C^1\sigma_3 = 1. \tag{3.2}$$

Symmetry requires that the oblique planes corresponding to the sides of "hexagon number one" are described by the equations shown in Table 1.

TABLE 1. EQUATIONS OF HEXAGONAL PYRAMIDS

Region	Side	Ordering of principal stresses	Equation	Eq. No.
I	$P_1^1Q_3^1$	$\sigma_1 > \sigma_2 > \sigma_3$	$A^1\sigma_1 + B^1\sigma_2 + C^1\sigma_3 = 1$	3.2-1
II	$P_2^1Q_3^1$	$\sigma_2 > \sigma_1 > \sigma_3$	$A^1\sigma_2 + B^1\sigma_1 + C^1\sigma_3 = 1$	3.2-2
III	$P_2^1Q_1^1$	$\sigma_2 > \sigma_3 > \sigma_1$	$A^1\sigma_2 + B^1\sigma_3 + C^1\sigma_1 = 1$	3.2-3
IV	$P_3^1Q_1^1$	$\sigma_3 > \sigma_2 > \sigma_1$	$A^1\sigma_3 + B^1\sigma_2 + C^1\sigma_1 = 1$	3.2-4
V	$P_3^1Q_2^1$	$\sigma_3 > \sigma_1 > \sigma_2$	$A^1\sigma_3 + B^1\sigma_1 + C^1\sigma_2 = 1$	3.2-5
VI	$P_1^1Q_2^1$	$\sigma_1 > \sigma_3 > \sigma_2$	$A^1\sigma_1 + B^1\sigma_3 + C^1\sigma_2 = 1$	3.2-6

Thus, we see that exactly three constants, A^1, B^1, C^1, are necessary and sufficient to define the six sides of the cross-section.

Similar reasoning shows that six constants A^2, B^2, C^2 are necessary and sufficient to define the six planes passing through the convex hexagon $P_1^2Q_3^2P_2^2Q_1^2P_3^2Q_2^2$. The equations for this second set of six space planes are found from Table 1, merely by replacing all superscript ones by superscript twos.

If the cross-section consisted of $6n$ sides, we would require $3n$ independent constants of the form:

$$A^j, B^j, C^j \qquad (j = 1 \ldots n).$$

The equations for the $6n$ space planes would be given as in Table 1, with the superscript 1 replaced by $j = 1, 2, \ldots n$, in succession.

It is apparent from equations (3.2) that each of the six planes passing through "hexagon number one" intersect at a common point where

$$\sigma_1 = \sigma_2 = \sigma_3 = 1/(A^1 + B^1 + C^1). \tag{3.3}$$

* Note that superscripts refer to a given pyramid, and subscripts refer to a given axis. The hexagon defined by superscript numeral j will be referred to as "hexagon number j".

In other words, the family of planes encloses a six-sided pyramid with a vertex on the hydrostatic axis.

The same remarks are true for each of the n hexagons which comprise the cross-section of the general piecewise linear failure surface. Thus, we may say that the generalized piecewise linear failure surface can be made up by adjoining sets of hexagonal pyramids. For this reason, we refer to such surfaces as "pyramidal failure surfaces".

4. THE HEXAGONAL PYRAMID FAILURE SURFACE

The simplest pyramidal failure surface is a single hexagonal pyramid. Although the Coulomb–Mohr pyramid belongs to this class of surfaces, it is a special case which suppresses many of the most interesting features of this class of surfaces because it requires one of the three disposable constants to be zero.

When all three disposable constants are allowed to assume non-zero values and the possibility of concavity is admitted, a rich variety of failure surfaces results, and hence a very wide variety of experimental results can be accommodated by a relatively simple theory.

Another motive for studying, the hexagonal pyramid failure surfaces arises from the fact that these pyramids represent, as we have seen, the building blocks from which the most general piecewise linear isotropic failure criterion can be built up.

The equations of the pyramid are given by equations (3.2), but since we are dealing with a single pyramid, we will omit the superscripts on the constants A^1, B^1, C^1 in what follows.

4.1 *Space equations in terms of strength parameters*

In order to express A, B, and C in terms of experimentally determinable properties, let us suppose that the material was observed to fail under stresses S_c, S_t and S_s in uniaxial compression, uniaxial tension, and pure shear, respectively.

Thus, the state of stress at failure in each case may be represented in the forms:

$$\text{Compression}: \sigma_1 = \sigma_2 = 0; \qquad \sigma_3 = -S_c \tag{4.1}$$

$$\text{Tension}: \sigma_1 = S_t; \qquad \sigma_2 = \sigma_3 = 0 \tag{4.2}$$

$$\text{Shear}: \sigma_1 = S_s; \qquad \sigma_2 = 0; \qquad \sigma_3 = -S_s. \tag{4.3}$$

In all the above cases, $\sigma_1 \geq \sigma_2 \geq \sigma_3$, hence equation (3.2-1) is the appropriate form to use in each case, and upon substitution of equations (4.1) and (4.2) into equation (3.2-1), it is found that

$$A = \frac{1}{S_t}; \qquad C = -\frac{1}{S_c}. \tag{4.4}$$

However, upon substitution of equation (4.3) into equation (3.2-1), it is found that

$$A - C = \frac{1}{S_s} = \frac{1}{S_t} + \frac{1}{S_c}. \tag{4.5}$$

In other terms, the state of pure shear provides no additional information for finding the constant B, but it does show that, according to this criterion, the failure stress in pure shear is related to the failure stress in pure compression and tension by the formula

$$S_s = \frac{S_c S_t}{S_c + S_t}. \tag{4.6}$$

It is readily verified that equation (4.6) is precisely the result predicted by Coulomb–Mohr theory, [8, p. 461].

In order to find the third constant, let us assume that the material was observed to fail at a stress S_v during a test under uniform triaxial tension. In other terms, put

$$\sigma_1 = \sigma_2 = \sigma_3 = S_v \tag{4.7}$$

into equation (3.2-1) to find

$$A + B + C = 1/S_v \tag{4.8}$$

hence:

$$BS_c = \frac{S_c}{S_v} - \frac{S_c}{S_t} + 1 = q - m + 1 \tag{4.9}$$

where we have used the notation:

$$q = S_c/S_v; \qquad m = S_c/S_t. \tag{4.10}$$

Coulomb–Mohr theory is a special case of this more general theory, wherein only the maximum and minimum principal stress can occur in the equation of a failure plane. In other words, the term B is identically zero in Coulomb–Mohr theory (see Table 1). We thus see from equation (4.9) that Coulomb–Mohr theory predicts failure under pure hydrostatic tension at a stress S_v given by

$$\frac{1}{S_v} = \frac{1}{S_t} - \frac{1}{S_c} \quad \text{(Coulomb–Mohr)}. \tag{4.11}$$

4.2 *Space equations in terms of pyramid parameters*

It may be seen from Fig. 4 that any given line such as $P_1^1 Q_3^1$ can be defined by its intersections with two axes in the deviatoric plane. For example, P_1^1 lies on the positive side of axis σ_1' and Q_3^1 lies on the negative side of axis σ_3'. The distances OP_1^1 and OQ_3^1 fully specify the line $P_1^1 Q_3^1$. Furthermore, since the space plane through $P_1^1 Q_3^1$ passes through a vertex point V, where $\sigma_1 = \sigma_2 = \sigma_3 = S_v^1$, the three distances OP_1^1, PQ_1^1, $OV = \sqrt{3}(S_v^1)$ uniquely fix the plane in question. Since OP_1^1 and OQ_1^1 completely define the base of a hexagonal pyramid, and $\sqrt{3}(S_v^1)$ is its altitude, we may speak of these three parameters as "pyramidal parameters".

It is shown in the Appendix (equations A3, A5) that

$$OP = \frac{\sqrt{6}}{(3/S_t) - (1/S_v)} \tag{4.12}$$

$$OQ = \frac{\sqrt{6}}{(3/S_c) + (1/S_v)}. \tag{4.13}$$

We have dropped the superscripts and subscripts in the above equations since all values of OP_j^i are equal for a given pyramid, likewise for all values of OQ_j^i.

Recalling from equation (4.4) that $A = 1/S_t$ and $-C = 1/S_c$, it proves desirable to solve equations (4.12) and (4.13) for $1/S_t$ and $1/S_c$ in the form:

$$A = 1/S_t = \frac{1}{3}\left(\frac{1}{S_v}+\frac{\sqrt{6}}{QP}\right) \tag{4.14}$$

$$C = -1/S_c = \frac{1}{3}\left(\frac{1}{S_v}-\frac{\sqrt{6}}{OQ}\right). \tag{4.15}$$

Finally, from equation (4.8) we can find

$$B = \frac{1}{S_v}-A-C = \frac{1}{3}\left(\frac{1}{S_v}+\frac{\sqrt{6}}{OQ}-\frac{\sqrt{6}}{OP}\right). \tag{4.16}$$

Thus, we obtain the three coefficients A, B, C of the space plane in terms of the pyramid parameters OQ, OP, S_v.

4.3 *Limitations on range of constants*

The equations of Table 1 predict a variety of failure surfaces, depending upon the relative values of the ratios $q = S_v/S_c$, and $m = S_c/S_t$. Let us confine our attention to the most important case where $S_c > S_t$, since most brittle materials are stronger in compression than they are in tension. Furthermore, let us assume that $S_v > 0$, since we would usually expect failure in hydrostatic tension rather than hydrostatic compression. It should be mentioned that $S_v < 0$ is by no means an impossibility. In fact, materials which fail in accordance with the maximum normal strain (or stress) criterion will have a failure surface which is the convex hull of two intersecting pyramids, one of which has a negative value of S_V.

For the sake of brevity, we will now assume that

$$m = (S_c/S_t) \geq 1 \tag{4.17}$$

$$q = S_c/S_v > 0. \tag{4.18}$$

Generalizations for other cases are quite straightforward.

It is immediately apparent from equation (4.12) that OP will be a positive quantity only if

$$3S_v > S_t; \qquad \text{i.e.: } q < 3m \tag{4.19}$$

Thus we see, that as long as we require S_v, S_t, and S_c to be positive quantities, it is necessary for S_v to exceed the value $S_t/3$ in order for the failure surface to enclose the origin in stress space.

From Fig. 4 it may be noted that the failure locus will be convex only if

$$OP_1^1 \geq OP_1^* = OQ_2^1 \sin 30° = OQ_1^1(1/2) \tag{4.20}$$

Upon substitution of equations (4.12, 4.13) into inequality (4.20), it will be seen that convexity requires

$$q \geq m - 2. \tag{4.21}$$

Similar reasoning shows that convexity requires

$$OQ_1^1 \geq OQ_1^* = OP_3^1 \sin 30° = OP_1^1(1/2)$$

or

$$q \leq 2m-1. \tag{4.22}$$

In short, the yield locus will be convex if, and only if, q lies in the interval

$$m-2 \leq q \leq 2m-1. \tag{4.23}$$

4.4 *Failure loci for plane stress*

If σ_3 is set equal to zero in equations (3.2), one obtains the six equations shown in Table 2.

TABLE 2. EQUATIONS FOR BIAXIAL STATES OF STRESS

Region	Equation	Slope $S = d\sigma_2/d\sigma_1$
I	$A\sigma_1+B\sigma_2 = 1$	$-A/B = m/(m-q-1)$
II	$A\sigma_2+B\sigma_1 = 1$	$-B/A = (m-q-1)/m$
III	$A\sigma_2+C\sigma_1 = 1$	$-C/A = \frac{1}{m}$
IV	$B\sigma_2+C\sigma_1 = 1$	$-C/B = \frac{1}{q+1-m}$
V	$B\sigma_1+C\sigma_2 = 1$	$-B/C = q+1-m$
VI	$A\sigma_1+C\sigma_2 = 1$	$-A/C = m$

In Table 2, equations (4.4) and (4.9) have been used to express the slope S in terms of m and q.

It turns out that there are five characteristic shapes of biaxial failure loci, which are readily drawn once one knows the general range of the slope $S = d\sigma_2/d\sigma_1$. The five possible cases are summarized in Table 3. Since the biaxial stress locus must be symmetrical about

TABLE 3. RANGE OF SLOPES FOR BIAXIAL STRESS LOCUS

Case	Range of q	Range of slope S in region			Remarks
		II	III	IV	
	$3m < q$				Inadmissible*
A	$2m-1 < q \leq 3m$	$-2-\frac{1}{m} \leq S < -1$	$\frac{1}{m}$	$\frac{1}{2m-1} \leq S < \frac{1}{m}$	Concave†
B	$m < q \leq 2m-1$	$-1 \leq S < -\frac{1}{m}$	$\frac{1}{m}$	$\frac{1}{m} \leq S < 1$	Convex‡
C	$m-1 < q \leq m$	$-\frac{1}{m} \leq S < 0$	$\frac{1}{m}$	$1 \leq S < \infty$	Convex‡
D	$m-2 < q \leq m-1$	$0 \leq S < \frac{1}{m}$	$\frac{1}{m}$	$-\infty \leq S < -1$	Convex‡
E	$q \leq m-2$	$\frac{1}{m} \leq S$	$\frac{1}{m}$	$-1 \leq S < 0$	Concave†

* Inadmissible by inequality (4.19).
† Inequality (4.23) violated.
‡ Inequality (4.23) satisfied.

the line $\sigma_1 = \sigma_2$, it is only necessary to record this information in three contiguous sectors such as II, III, IV. After drawing the locus in the region $\sigma_2 > \sigma_1$, the other half of the curve is found by reflection about the line of symmetry.

Figures 5 A–E show all possible varieties of biaxial failure loci for the six sided pyramid with $S_c > S_t > 0$; and $S_v > 0$.

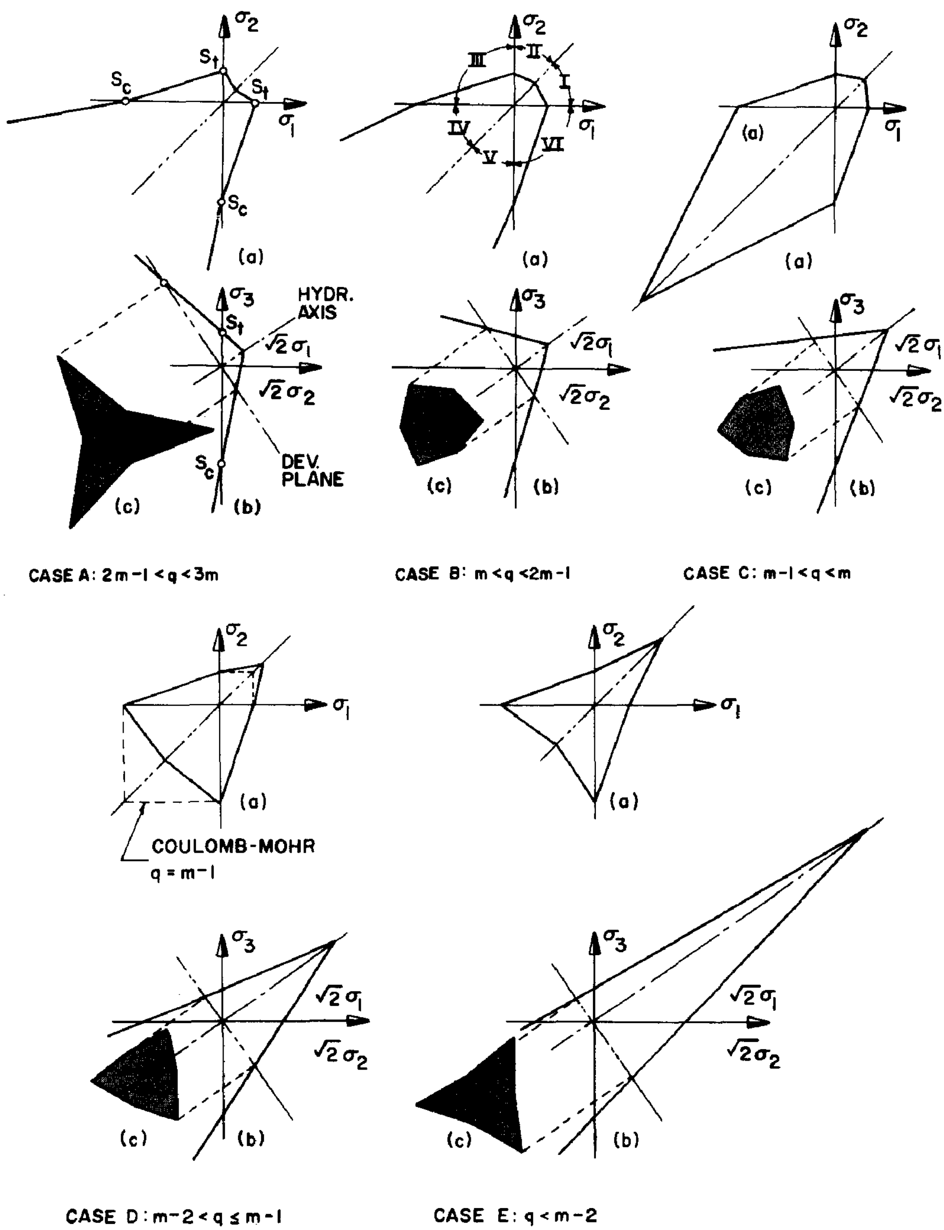

FIG. 5. Showing all possible failure loci for: (a) biaxial stress, (b) confined pressure, (c) cross-section through deviatoric plane.

It is of interest to note that the Coulomb–Mohr criterion (shown as a limiting case of Fig. 5D) predicts a closed biaxial failure locus, whereas the more general criterion of this Section predicts both open and closed loci, which may be either convex or concave, depending upon the range of parameters used. It is also of interest that this three-parameter criterion is capable of describing such a wide variety of material behavior; and that the effect of the intermediate principal stress can theoretically exert a profound influence on the shape of the failure surface.

5. KNOWN SPECIAL CASES

Many of the yield and fracture surfaces suggested over the years for various materials are special cases of the generalized pyramidal surface. Listed below are several of the known surfaces of this type.

(i) *The Coulomb–Mohr surface* [30, 31, 32] is a special case of the generalized pyramidal failure surface, consisting of a single pyramid, each of whose sides is parallel to one of the coordinate axes. That is, the Coulomb–Mohr surface is completely described by equation (3.2) with

$$B^1 = 0.$$

(ii) *The Tresca* [11] criterion (see Fig. 2) is a special case of Coulomb–Mohr theory with the vertex of the pyramid infinitely far from the origin.

(iii) *The Coulomb–Mohr criterion with tension cutoffs* [5] is a pyramidal yield criterion wherein the Coulomb–Mohr pyramid is intercepted by a second pyramid (see Fig. 6).

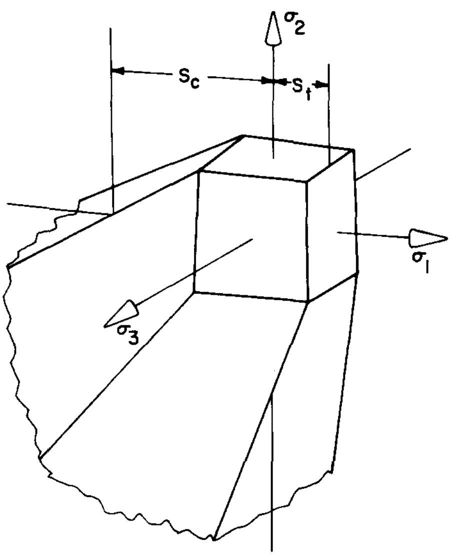

FIG. 6. Coulomb–Mohr criterion with tension cutoff.

This latter pyramid, representing the tension cutoffs, is another special case of the general hexagonal pyramid wherein two sides (such as $Q_3^2P_1^2$ and $P_1^2Q_2^2$ in Fig. 4) merge to form a triangular cross section. Cowan [33] has suggested tension cutoffs of a slightly different nature, and Drucker [34] had suggested that no tension was possible (zero cutoffs) for a particular pyramid which is a generalized Tresca cylinder.

(iv) *The maximum normal stress* criterion is a special case in which two triangular pyramids, with vertices on opposite sides of the origin intersect to form a cube.

(v) *The maximum normal strain* criterion of St. Venant [35] is another case where two triangular pyramids merge to form an oblique parallelepiped; see Fig. 7 taken from Westergaard [36].

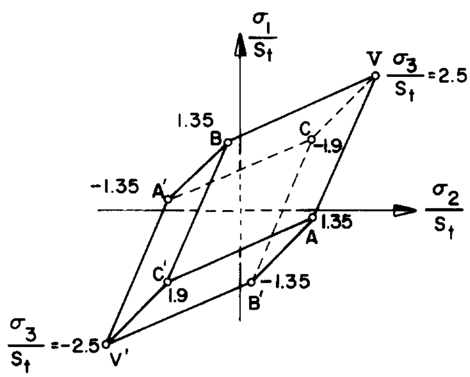

FIG. 7. Maximum normal strain criterion, union of pyramids $VABC$ and $V'A'B'C'$. Projection on plane $\sigma_3 = 0$; numbers indicate values of σ_3/S_t, after Westergaard [36].

(vi) *The Von Mises* [12] criterion (see Fig. 2) is the only widely used failure criterion for isotropic materials which is not piecewise linear. However, it may be approximated to any desired degree of accuracy by a regular polygonal cylinder with a large number of sides. Such a cylinder would also be a pyramidal failure surface, with the vertex of each pyramid infinitely far from the origin.

(vii) *Generalizations of Von Mises and Tresca criteria.* The circular cylinder of Von Mises can be generalized to a circular cone, as discussed by Nadai [1, p. 227] and Drucker and Prager [37]. A pyramidal approximation to this circular cone was discussed by Drucker [34] who viewed the pyramid as a generalization of the Tresca criterion. Paraboloidal generalizations of the Von Mises criterion, were discussed by Nadai [1, p. 227] and Stassi-D'Alia [38]. Civil Engineering literature on soils and concrete [39, 40] abounds in discussions of the conical and paraboloidal failure surfaces, although not necessarily referred to as such. Murrell [41] has suggested a paraboloid joined to a triangular pyramid which forms a maximum tension "add-on", for use with natural rocks.

(viii) *Becker's criterion.* Westergaard [36] felt that the weight of evidence, at the time, favored acceptance of a criterion advanced by Becker [42] for yielding of steels. The corresponding failure surface is the convex hull of Tresca's cylinder and St. Venant's double pyramid (parallelepiped). This special case of the generalized pyramidal failure criterion is now of historical interest only, but it did provide the motivation for Westergaard's often quoted paper [36].

(ix) *Haythornthwaite* [20] coined the expression "*maximum reduced stress criterion*" for the case where the yield surface is a regular hexagonal cylinder which would circumscribe the Tresca cylinder if both surfaces passed through the points in stress space representing pure tension and pure compression. He also pointed out that the maximum reduced stress cylinder could be generalized into what we have here termed a pyramidal failure surface in the same way that Tresca's hexagon is generalized into Coulomb–Mohr's pyramid. Haythornthwaite [20] also discussed generalizations of the Coulomb–Mohr and reduced stress failure criteria which are special cases of the generalized pyramidal failure criterion.

6. APPLICATIONS TO REAL MATERIALS

In the previous sections it was shown that the generalized pyramidal failure surface is capable of describing any isotropic material which yields or fractures in accordance with a macroscopic stress criterion. It was also shown that certain special cases can represent a wide variety of material behavior patterns with just a few experimental constants. For example, the hexagonal pyramid needs three parameters; its special case, the Coulomb–Mohr pyramid, needs only two parameters; tension cutoffs introduce another parameter, and so on. The pyramidal criteria will prove to be useful only if the simple (few parameter) variants are capable of describing real materials.

In the following sections, it will be shown that a great deal of experimental evidence exists which indicates that the brittle fracture or yielding of a very wide class of materials can be well described by a pyramidal failure criterion. It will be noted that these materials are pressure-dependent and generally are influenced by the intermediate principal stress, at failure.

Only a sampling of the vast literature in this field can be offered here. One example will be given of experimental results from each of four classes of pressure-dependent materials. Additional examples and references to experiments are given in [6]. Space does not permit an adequate discussion of the accuracy and experimental validity of the work discussed. Nevertheless, it is believed that, on balance, the available evidence clearly points to the advantages of pyramidal criteria for describing the behavior of materials.

6.1 *Brittle metals*

The data of Coffin [43], shown in Fig. 8, represents one of the few instances where experiments have been made in the compression–compression quadrant. If the Coulomb–Mohr criterion were valid in this quadrant, the fracture curve would consist of two lines, respectively parallel to the coordinate axes as shown by the dotted lines in Fig. 5D. The fact is that the experimental points lie on a sloping line, which indicates that a hexagonal pyramidal fracture locus of the type shown in Fig. 5C might be applicable. The slope of the heavy line drawn through the data points is approximately 0·36. For $m = 2{\cdot}04$, as indicated in the fourth quadrant of Fig. 10, we can find the parameter q from the fifth equation of Table 2, in the form:

$$q = S+m-1 = 0{\cdot}36+2{\cdot}04-1 = 1{\cdot}40.$$

The slope of the pyramidal failure locus in the first quadrant, is given by line 1 of Table 1, in the form:

$$S = m/(m-q-1) = 2{\cdot}04/(2{\cdot}04-1{\cdot}40-1) = -5{\cdot}65.$$

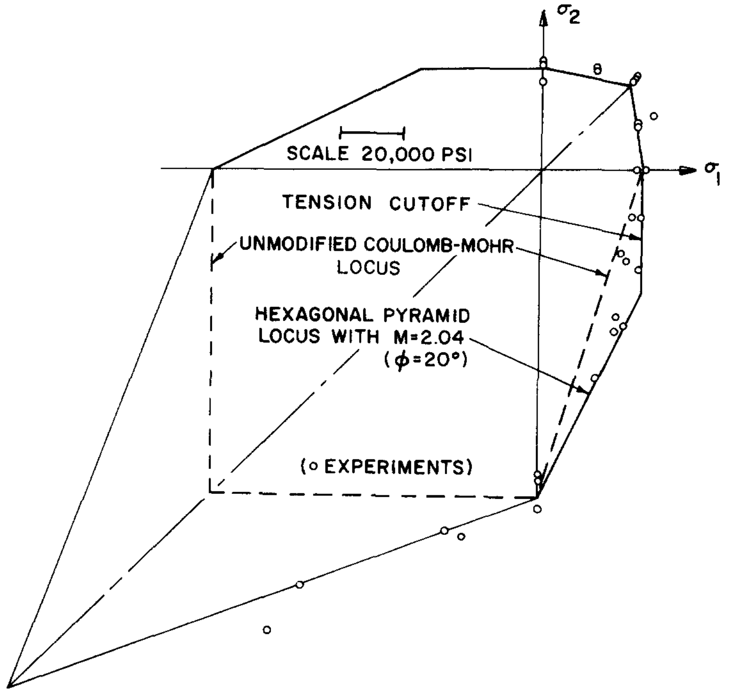

FIG. 8. Data of Coffin [43] on gray cast iron fitted by pyramidal criterion with $m = 2{\cdot}04$, $q = 1{\cdot}40$.

The above value has been used to draw the portion of the fracture locus in the first quadrant. It is seen that a hexagonal pyramid (with, or without tension cutoffs) describes the major features of the fracture locus for this Cast Iron under biaxial stress. In order to evaluate the need for such a generalization of the Coulomb–Mohr criterion, it is important to know whether the experimental points, shown in the third quadrant, represent true biaxial stress states, or if they represent states with three non-zero principal stresses (a possibility suggested in [5]). This question could theoretically be resolved by finding additional points in region IV, where $0 > \sigma_2 > \sigma_1$.

6.2 *Soils*

The most common test for determining the failure criterion for a granular material is the confined compression or so-called "triaxial test". Although such a test is capable of ruling out the possibility that the Coulomb–Mohr (or any other hexagonal pyramid) criterion is applicable, it cannot confirm that such criteria are valid because these tests only provide two points when projected centrally onto an equipressure plane. More general tests such as torsion–compression or compression–compression on hollow cylinders are required to trace out the true locus on a typical equipressure plane. Such tests, although an improvement on the confined pressure tests are limited because they are essentially plane stress types of tests. Some recent experiments, where all three principal stresses were varied independently, indicate that, although the time-honored Coulomb–Mohr criterion represents a reasonable first approximation for many soils, there is a very definite influence of intermediate principal stress, which is not accounted for by the

Coulomb–Mohr criterion. Several previous authors, who have discussed this point, have suggested that the failure criterion should be expressed in terms of the second, and possibly, the third, invariant of the stress tensor in order to include such effects. However, in the experimental data which the author has seen, some of which is presented below, a pyramidal failure criterion is at least equally, reasonable from a practical viewpoint.

Shibata and Karube [44] have modified the standard "triaxial cell" in such a way as to be able to independently vary the intermediate principal stress. Figure 9 shows their data, projected centrally from a postulated vertex point, onto an equipressure plane (the influence of pore water pressure has been subtracted out). It is seen that there must be an

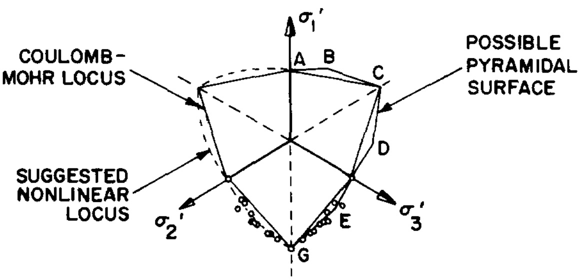

FIG. 9. Experimental data of Shibata and Karube [44] for normally consolidated clay (effective stresses shown).

effect of intermediate principal stress since the data points do not lie on the Coulomb–Mohr locus. Shibata and Karube suggest that the data should be correlated by the dotted curve shown on the left hand side of the Figure (only half of the symmetric locus is shown). The polygon on the right hand side represents an equally acceptable pyramidal type of failure criterion. Sides such as *ED* may be interpreted as tension cutoffs (possibly pressure-dependent cutoffs) which intercept a hexagonal pyramid.

6.3 *Dry granular media*

Lenoe [45] constructed apparatus for independently varying any one of the three principal stresses acting on a granular sample, and has used it to find the failure criterion for a mixture of sand, silt, and gravel. He concludes that the intermediate principal stress plays a significant role in the failure criterion and suggests that his data can be correlated by a failure criterion of the form $J_2 = 160+0{\cdot}223\, J_3$ or $J_1 = 21{\cdot}5+0{\cdot}0535\, J_2$, where J_1, J_2, J_3 are the first three variants of the stress tensor.

However, it is hardly necessary to resort to nonlinear criteria because the data can be satisfactorily correlated by a hexagonal pyramid failure criterion, whose equation is

$$2\sigma_1+4\sigma_2-\sigma_3 = 0; \qquad (\sigma_1 \leq_2 \ \leq \sigma_3)$$

Lenoe's data is replotted in Fig. 10, where it may be seen that all points, with the exception of one (marked point A in Fig. 10) fall within 5 % of the ordinate value predicted by the above equation.

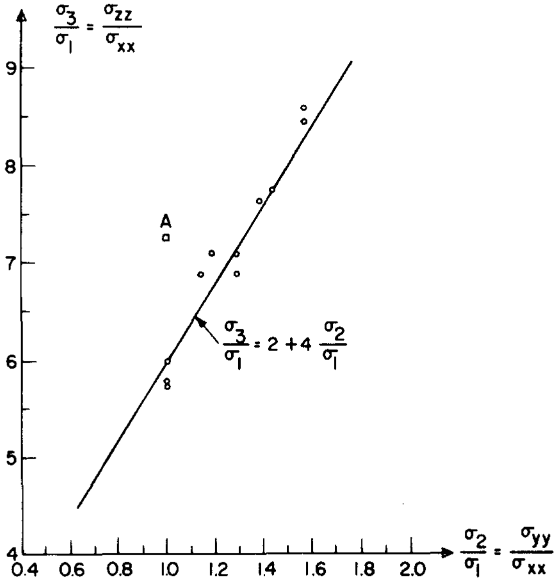

FIG. 10. Data of Lenoe [45] on dry cohesionless soil.

6.4 *Rocks*

In recent years there has been an upsurge of interest in the failure characteristics of rocks. Space prohibits a detailed discussion of this work, but excellent recent bibliographies, such as that of Bieniawski [46] are available. A comprehensive view of this field will be found in the survey by Jaeger [4], and in collections and symposia, such as those edited by Griggs and Handin [47], and Fairhurst [48].

Numerous experiments on rocks, which are described in the general references mentioned above, show the existence of tension cutoffs and imply the possibility of a hexagonal pyramidal failure surface. A recent example of such experiments is shown in Figs. 11 and 12.

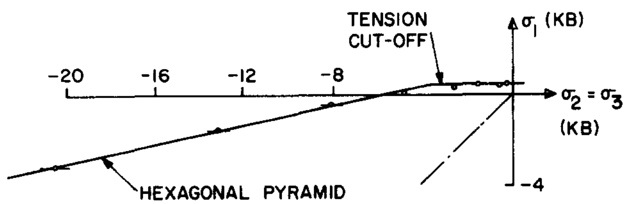

FIG. 11. Fracture locus of diabase in confined compression plane. Data from Brace [49].

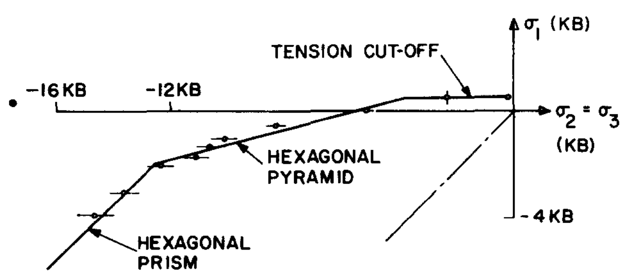

FIG. 12. Fracture locus of Blair dolomite in confined compression plane. Data from Brace [49].

The data shown were obtained by Brace [49] in confined compression and confined tension tests. Figure 11 indicates that a simple hexagonal pyramid with tension cutoffs would be adequate for the diabase rock tested, over the range of mean pressure tested, whereas Fig. 12 indicates that the same type of failure surface would be valid, for the dolomite tested at low mean pressures, but it would be superseded by a Tresca type cylinder at high mean pressures.

7. CONCLUSIONS

Formulation of failure criteria in terms of simple variants of the generalized pyramidal failure surface is convenient, flexible, and sufficiently accurate for an extremely wide class of pressure-dependent materials, including brittle metals, soils, rocks, and dry granular media. Most of the failure criteria proposed in the past can be interpreted as special cases of pyramidal criteria. Finally, previously proposed criteria, which are essentially extensions of Von Mises' criterion (or other nonlinear criteria involving stress invariants), do not correlate the known experimental data any better than do simple versions of the pyramidal criteria, which have the advantage of being piecewise-linear.

REFERENCES

[1] A. Nadai, *Theory of Flow and Fracture of Solids*. McGraw-Hill (1950).
[2] K. Terzaghi, *Theoretical Soil Mechanics*. Wiley (1943).
[3] R. F. Scott, *Principles of Soil Mechanics*. Addison-Wesley (1963).
[4] J. C. Jaeger, Brittle fracture of rocks, *Proc. 8th Symp. Rock Mechanics*, Sept. 1966, edited by C. Fairhurst. Am. Inst. Min. metall. Petrol. Engrs, 3-57 (1967).
[5] B. Paul, A modification of the Coulomb–Mohr theory of fracture. *J. appl. Mech.* **28**, 259–268 (1961).
[6] B. Paul, Macroscopic criteria for plastic flow and brittle fracture. *Treatise on Fracture*, edited by H. Liebowitz. Academic Press. (To be published.)
[7] R. Hill, *The Mathematical Theory of Plasticity*. Oxford University Press (1950).
[8] S. Timoshenko, *Strength of Materials*, Part II, 3rd edition. Van Nostrand (1956).
[9] D. C. Drucker, A more fundamental approach to plastic stress–strain relations. *Proc. 1st U.S. Natn. Congr. appl. Mech.* Published by ASME, pp. 487–491 (1952).
[10] J. F. W. Bishop and R. Hill, A theory of the plastic distortion of a polycrystalline aggregate under combined stresses. *Phil. Mag.* **42**, 414–427 (1951).
[11] H. Tresca, Sur l'écoulement des corps solides soumis à les fortes pressions. *C.R. hebd. Séanc. Acad. Sci., Paris* **59**, 754–758 (1864); **64**, 89 (1867).
[12] R. von Mises, Mechanik der festen Koerper im Plastisch deformablen Zustand. *Nachr. Ges. Wiss. Gottinger* 582–592 (1913).
[13] J. C. Maxwell, Letter to Lord Kelvin, Dec. 18, 1856. Pertinent portion of letter quoted by Nadai, *Theory of Flow and Fracture of Solids*, Vol. II, p. 43. McGraw-Hill (1963).
[14] M. T. Huber, A contribution to fundamentals of the strength of materials (in Polish). *Czas. Tow. tech. krakow* **22**, 81 (1904).
[15] H. Hencky, Zur Theorie plastischen Deformationen und hierdurch im Material hervorgerufenen Nebenspannungen. *Proc. 1st Int. Congr. appl. Mech.* Delft, 312–317 (1924).
[16] A. Nadai, Theories of strength. *J. appl. Mech.* **1**, 111–129 (1933).
[17] D. C. Drucker, Stress–strain relations in the plastic range. *Brown Univ. Rep.* A11-S1 to ONR, (1950).
[18] D. C. Drucker, Stress–strain relations in the plastic range of metals—experiments and basic concepts. *Rheology, Theory and Applications*, edited by F. R. Eirich, Vol. 1, pp. 97–119. Academic Press (1956).
[19] D. D. Ivlev, On the development of a theory of ideal plasticity. *Prikl. Mat. Mekh.* **22**, 850–855 (1958); *PMM* 1221–1230 (English transl.).

[20] R. M. HAYTHORNTHWAITE, Range of yield condition in ideal plasticity. *Trans. Am. Soc. civ. Engrs* **127**, Part I, 1252–1267 (1962).
[21] W. PRAGER, On the use of singular yield conditions and associated flow rules. *J. appl. Mech.* **20**, 317–320 (1953).
[22] W. PRAGER, A new method of analyzing stresses and strains in work-hardening plastic solids. *J. appl. Mech.* **23**, 493–496 (1956).
[23] W. T. KOITER, Stress–strain relations, uniqueness and variational theorems for elastic–plastic materials with a singular yield surface. *Q. appl. Math.* **11**, 350–354 (1953).
[24] J. L. SANDERS, JR., Plastic stress–strain relations based on linear loading functions. *Proc. 2nd U.S. Congr. appl. Mech.*, 455–460 (1955).
[25] P. G. HODGE, JR., A general theory of piecewise linear plasticity based on maximum shear. *J. Mech. Phys. Solids* **5**, 242–260 (1957).
[26] R. T. SHIELD and H. ZIEGLER, On Prager's hardening rule. *Z. angew. Math. Phys.* **9a**, 260–276 (1958).
[27] N. PERRONE and P. G. HODGE, JR., Strain hardening solutions with generalized kinematic models. *Proc. 3rd U.S. Natn. Congr. appl. Mech.*, 641–648 (1958).
[28] I. BERMAN and P. G. HODGE, A general theory of piecewise linear plasticity for initially anisotropic materials. *Archwm Mech. stosow.* **11**, 513–539 (1959).
[29] B. PAUL, Plastic and viscous deformation of redundant structures—prototypes for a general theory. *J. Franklin Inst.* **273**, 482–514 (1962).
[30] C. A. COULOMB, Sur une application des régles de maximis et minimis à quelques problèmes de statique, relatifs à l'Architecture. *Mèm. Math. Phys.* **7**, 1773, 343 Academie Royal des Sciences, par divers Savans (1776).
[31] O. MOHR, Welche Umstände bedingen die Elastizitätsgrenze und den Bruch eines Materials? *Z. Ing.* **44**, 1524–1530 (1900).
[32] J. GUEST, The strength of materials under combined stress. *Phil. Mag.* **50**, 69–132 (1900).
[33] H. J. COWAN, The strength of plain, reinforced and prestressed concrete under the action of combined stresses, with particular reference to the combined bending and torsion of rectangular sections. *Mag. Concr. Res.* **5**, 75–86 (1953).
[34] D. C. DRUCKER, Limit analysis of two and three dimensional soil mechanics problems. *J. Mech. Phys. Solids* **1**, 217–226 (1953).
[35] B. SAINT-VENANT, Lecons de mécanique appliquée faites par intérim par M. de St-Venant, Ingénieur des ponts et chausées. 1837 à 1838, unpublished course of lectures, lithographed; referred to by TODHUNTER and PEARSON, *History of Elasticity*, Vol. I, p. 831. Cambridge (1886).
[36] H. M. WESTERGAARD, The resistance of ductile materials to combined stresses in two or three directions perpendicular to one another. *J. Franklin Inst.* **189**, 627–640 (1920).
[37] D. C. DRUCKER and W. PRAGER, Soil mechanics and plastic analysis or limit design. *Q. appl. Math.* **10**, 157–165 (1952).
[38] F. STASSI-D'ALIA, *Teoria della plasticita e sue applicazioni.* (A volume of XII) edited by G. DENARO, Palermo, Italy, (1958). Quoted by author in *A limiting condition of yielding and its experimental confirmation.* Instituto di Tecnologie Meccaniche della Universita' di Palermo (Facolta d'Ingegneria), N.D. (16 pp).
[39] B. BRESLER and K. S. PISTER, Failure of plain concrete under combined stresses, *Trans. Am. Soc. civ. Engrs* **122**, 1049–1068 (1957).
[40] B. BRESLER and K. S. PISTER, Strength of concrete under combined stresses. *J. Am. Concr. Inst.* **30**, 321–345 (1958); discussion in **30**, 1035–1046 (1958).
[41] S. A. F. MURRELL, A criterion for brittle fracture of rocks and concrete under triaxial stress, and the effect of pore pressure on the criterion. *Proc. 5th Symp. Rock Mechanics* held at the Univ. of Minnesota, May 1962; published in *Rock Mechanics*, edited by C. FAIRHURST, pp. 563–577. Pergamon Press (1963).
[42] A. J. BECKER, The strength and stiffness of steel under biaxial loading. *Bull. Ill. Univ. Engng Exp. Stn.* **85** (1916).
[43] L. F. COFFIN, The flow and fracture of brittle material. *J. appl. Mech.* **17**, 233–248 (1950).
[44] T. SHIBATA and D. KARUBE, Influence of the variation of the intermediate principal stress on the mechanical properties of normally consolidated clays. *Proc. 6th Int. Conf. Soil Mech. Foundation Engng*, Vol. I, pp. 359–363. University of Toronto Press (1965).
[45] E. M. LENOE, Deformation and failure of granular media under three-dimensional stresses. *Expl. Mech.* **6**, 99–104 (1966).
[46] E. M. BIĘNIAWSKI, A bibliography on fracture of rock, CSIR Report No. MEG 355, Pretoria, South Africa, National Mechanical Engineering Research Institute, Council for Scientific and Industrial Research, May (1965).
[47] D. GRIGGS and J. HANDIN, Rock deformation. *Mem. geol. Soc. Am.* **79** (1960).
[48] C. FAIRHURST, *Proc. 8th Symp. Rock Mechanics*, edited by C. FAIRHURST, Am. Inst. Min. metall. Petrol. Engrs (1967).
[49] W. F. BRACE, Brittle fracture of rock. *State of Stress in the Earth's Crust*, edited by W. R. JUDD, pp. 111–178. Elsevier (1964).

APPENDIX

In order to express the "pyramidal parameters" OP and OQ in terms of material strength parameters S_t, S_c, and S_v, it is convenient to consider the locus obtained in a "confined compression test" in which two of the principal stresses (say σ_1 and σ_2) are equal. The plane $\sigma_1 = \sigma_2$ intersects the space pyramid in two straight lines which emanate from the vertex V, as shown in Fig. 13, and pass through the axis of σ_3 at points T and C which

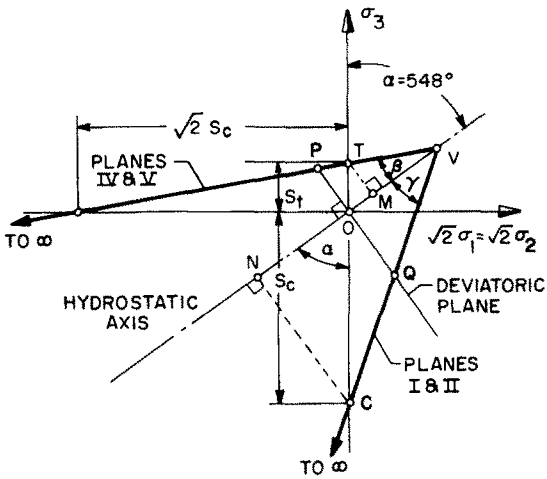

FIG. 13. Locus of "confined compression test" ($\sigma_1 = \sigma_2$) corresponding to pyramidal criterion.

are distances $OT = S_t$, and $OC = S_c$. The trace of deviatoric plane is perpendicular to the hydrostatic axis OV, and intersects the lines VT and VC at the points P and Q (corresponding to points such as P_3^2 and Q_3^2 in Fig. 4), respectively.

From Fig. 13, it is seen that

$$OP = OV \tan\beta = \sqrt{3}S_v \tan\beta \tag{A1}$$

where use has been made of the fact that

$$OV = \sqrt{(S_v^2 + S_v^2 + S_v^2)} = \sqrt{3}S_v.$$

In order to find $\tan\beta$, we note, from triangle TMV, that

$$\tan\beta = \frac{MT}{MV} = \frac{OT\sin\alpha}{OV - OM} = \frac{S_t \sin\alpha}{\sqrt{3}S_v - S_t\cos\alpha} \tag{A2}$$

Upon noting that $\cos\alpha = 1/\sqrt{3}$, $\sin\alpha = \sqrt{(2/3)}$, and using equation (A2), we can write equation (A1) in the form

$$OP = \frac{\sqrt{6}(S_v S_t)}{3S_v - S_t} = \frac{\sqrt{6}}{(3/S_t) - (1/S_v)} \tag{A3}$$

In a similar fashion, we find that

$$\tan\gamma = \frac{NC}{NV} = \frac{OC\sin\alpha}{OV + ON} = \frac{S_c\sin\alpha}{\sqrt{3}(S_v) + S_c\cos\alpha} \tag{A4}$$

$$OQ = OV\tan\gamma = \frac{\sqrt{6}(S_v S_c)}{3S_v + S_c} = \frac{\sqrt{6}}{(3/S_c) + (1/S_v)} \tag{A5}$$

(*Received* 7 *February* 1967; *revised* 1 *June* 1967)

Абстракт—Обобщенное условие разрушения в виде пирамиды является очень пригодным для описания напряженного состояния, под влиянием которого изотропные материалы будут проявлять

течение при хрупком изломе. Общий вид условия очень удобный для весьма сложных материа лов, но предполагается, что большинство материалов может быть описано равнозначно простыми вариантами этого общего условия. Оказывается например, что условие в виде гексагональной пирамиды, как специальный случай более общего условия в виде пирамиды, является пригодным для описания поведения очень широкого круга материалов, используя только три параметры, которые вытекают из опыта. Приводится применение условия в виде пирамиды к действительным материалом на основе обзора экспериментальных результатов, проведенных на хрупких металлах, бетонах, натурных горных породах, материалах и грунтах.